

Design of planar coils of minimum resistance for magnetic recording devices

Problem presented by
Ferdinand Hendriks
IBM Research Division
T. J. Watson Research Center
Hawthorne, NY

Participants:	M. Bousquet	R. Buckmire	P. Howell
	J. King	L. Kunyansky	N. Nigam
	T. Peterson	C. Please	P. Plechac
	Rakesh	R. Sipcic	I. Stakgold
	T. Ueda	J. Vail	T. Witelski

Report by T. Witelski

1 Introduction

Magnetic data stored on computer hard disk drives is read and written by small electromagnets on read/write heads that pass over the surfaces of the spinning hard disks [7]. These electromagnets are composed of magnetic alloy cores with wire coils wrapped around them. When an electric current is sent to the coil, a magnetic field is induced in the ferrite core, and data is written to the disk by changing the magnetization of data bits on the disk. One class of read-write heads, called thin-film heads, uses a two-dimensional spiral path of conducting material on an insulating substrate as the induction coil surrounding the horseshoe-shaped ferrite core (see Figure 1).

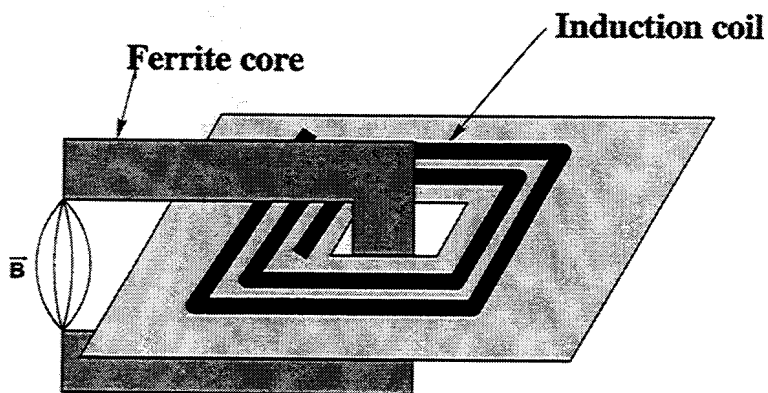


Figure 1: Schematic illustration of the induction coil surrounding the ferrite core in a thin film write head.

Increases in the speed and storage density of hard disk drives can be achieved by improvements in the design and response speed of the read/write head. The speed at which data bits can be written to the disk surface is limited by the electrical characteristics of the ferrite core and the induction coil. A full simulation of the behavior of writing a data bit would involve computations of transient high frequency behavior. We propose progress in the design of thin film induction coils by solving a steady

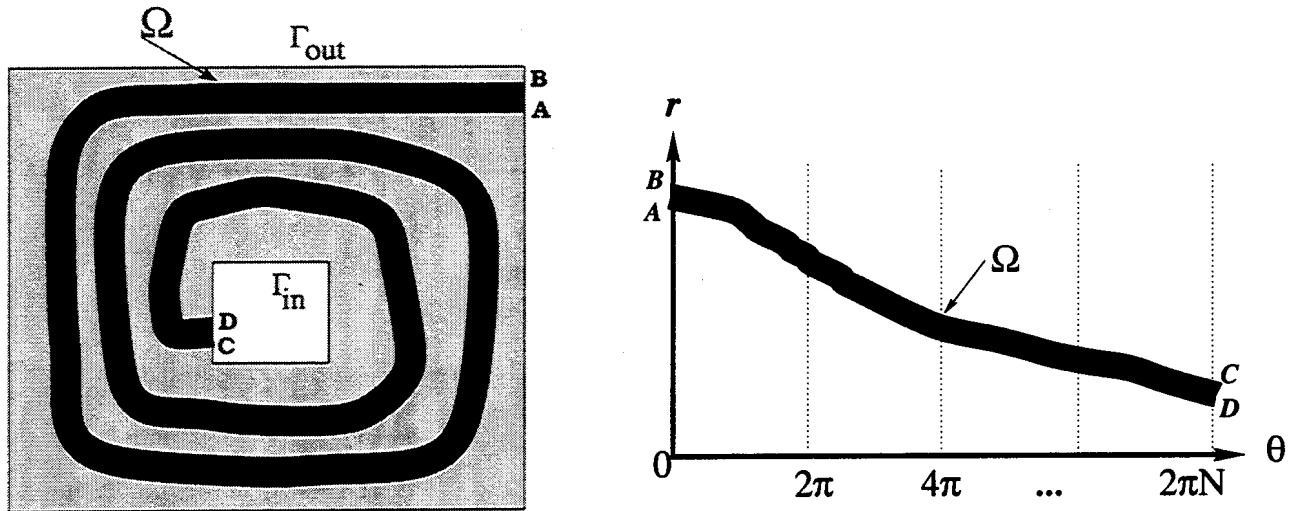


Figure 2: [Left] (a) The geometry of the free boundary problem for the coil shape. [Right] (b) Representation of the problem for a coil with N turns in polar coordinates.

problem to minimize the resistance of the coil.

To achieve the desired induced magnetic field in the ferrite core, the induction coil must have a certain number of turns, N , around the core. From classical electromagnetism [1, 6], the intensity of the induced magnetic field is proportional to the product of the number of turns, N , and the current in the wire, I . For a fixed given current and a fixed typical number of turns, $N = 10$, the power consumption of the induction coil will be minimized by minimizing its resistance.

2 Problem formulation

Electrostatic fields in homogeneous, isotropic conductors are given by solutions of Laplace's equation [1]. Our problem for the design of a thin film induction coil with minimum resistance can be expressed mathematically as a free boundary problem for Laplace's equation in an annular domain, \mathcal{D} , bounded by the inner and outer curves Γ^{in} and Γ^{out} (see Figure 2a). The shape of the coil will be a simply connected domain, $\Omega = ABCD$, that will be determined as the solution of this problem. The coil shape Ω is subject to several geometric constraints;

1. Ω must lie inside the annular domain \mathcal{D} between Γ^{out} and Γ^{in} ,
2. $\partial\Omega$ must include the segment AB of Γ^{out} (a fixed connection to a current source),
3. $\partial\Omega$ must include the segment CD of Γ^{in} (a fixed connection to a current sink),
4. Ω must make the desired number of complete turns, N , around Γ^{in} .
5. An additional constraint on the shape of Ω is given by manufacturing and physical considerations. Clearly, Ω should not self-intersect (to avoid short-circuits), moreover, the turns of Ω must be separated in the plane by at least distance δ . This condition, called a lithographic constraint, defines the resolution of the process of depositing conducting material on the insulating substrate. Below the scale of δ , the edges of Ω will not be well-resolved. Hence turns closer together than δ may produce short circuits or other undesirable electrical coupling effects (like capacitance).

Physically, AB and CD represent the beginning and ending points of the coil, where it will be attached to the rest of the electrical circuit elements in the read/write head. The region given by Ω will be assumed to have a uniform conductivity, while the surrounding regions are all perfectly insulating. Therefore, apart from AB and CD , the rest of $\partial\Omega$ will carry no flux of current. To define the electrical resistance of the coil, we apply a unit voltage difference, and obtain the electrostatic potential field in the coil, $\phi(x, y)$ (see Figure 2),

$$\nabla^2\phi = 0 \quad \text{on } \Omega \quad (1)$$

$$\phi = 1 \quad \text{on } AB \quad (2)$$

$$\phi = 0 \quad \text{on } CD \quad (3)$$

$$\mathbf{n} \cdot \nabla\phi = 0 \quad \text{on the rest of } \partial\Omega \quad (4)$$

Given the domain Ω , equations (1–4) specify a well-posed problem with a unique solution. While the formulation (1–4) does not specify the number of turns, N , this constraint can be made explicit by expressing the problem in terms of polar coordinates, (r, θ) (see Figure 2b). For a free-boundary problem we need an additional equation to determine Ω ; this extra condition will be the maximization of the current through CD ,

$$I = \max_{\Omega} \int_{CD} \mathbf{n} \cdot \nabla\phi \, ds, \quad (5)$$

where the maximization is carried out over the set of Ω 's that satisfy all of the geometric constraints given above. By conservation of charge, the current I is also equal to the current into Ω through AB , $I = -\int_{AB} \mathbf{n} \cdot \nabla\phi \, ds$. Using Green's first identity [10],

$$\int \int_{\Omega} \nabla f \cdot \nabla g \, dA + \int \int_{\Omega} f(\mathbf{x}) \nabla^2 g \, dA = \int_{\partial\Omega} f(\mathbf{x}) (\mathbf{n} \cdot \nabla g) \, ds, \quad (6)$$

with $f = g = \phi(x, y)$, we can also express the current for a domain with a unit potential difference as

$$I = \int \int_{\Omega} |\nabla\phi|^2 \, dA. \quad (7)$$

For a coil composed of a long slender wire, we can estimate the magnitude of I from dimensional analysis. If the length of the coil is $L \sim 2\pi N$, and it has a uniform width $W \sim \alpha \bar{W}/N$, where \bar{W} is a characteristic width between Γ^{in} and Γ^{out} , then

$$I \sim \left(\frac{1}{L}\right)^2 LW = \frac{W}{L} = \frac{\alpha \bar{W}}{2\pi N^2}. \quad (8)$$

The parameter α , $0 < \alpha < 1$, gives a measure of how much of the domain \mathcal{D} is taken up by the coil, $\alpha = \text{area}(\Omega)/\text{area}(\mathcal{D})$. From (8), it is clear that the current can be maximized by using all of the available area for the coil, up to the lithographic constraint, $\alpha = 1 - O(2\pi N\delta)$. As the number of turns, N , is increased, the current is decreased, but for any fixed N there should be a coil design that achieves a maximum current flow.

In practice, we approached the problem of coil shape optimization [8] by minimizing resistance instead of maximizing current flow. For a unit potential difference across Ω , the resistance of the coil is given by $R = 1/I$, hence maximizing the current is equivalent to minimizing the resistance. By treating each coil turn as a lumped circuit element with an effective resistance, R_i , $i = 1, 2, \dots, N$, we can obtain the total resistance of the coil from the turns connected in series, $R = R_1 + R_2 + \dots + R_N$ (see

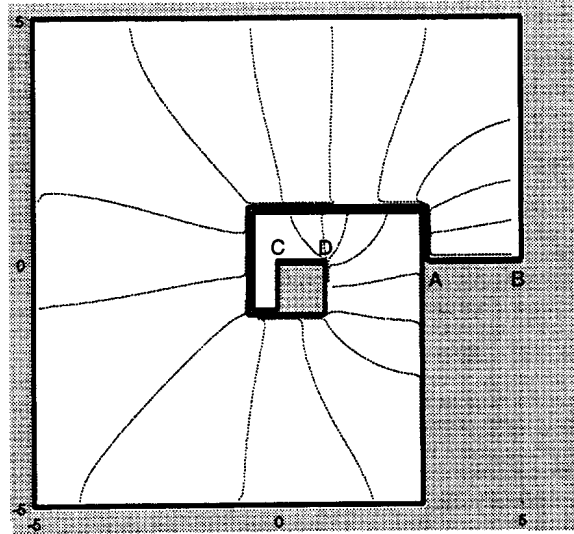


Figure 3: A boundary element method (BEM) calculation of the lines of constant potential in a one-turn coil. This coil is near-optimal in the restricted two-parameter set of designs with piecewise constant boundaries.

Figure 2b). For rectangular strips, the resistance is proportional to the ratio of the length to the width, $R = L/W$. This expression for the resistance can be shown to generalize for all geometries through the use of potential theory [2, 4]. The harmonic conjugate of $\phi(x, y)$, $\psi(x, y)$, makes the combination $f(z) = \phi(x, y) + i\psi(x, y)$ an analytic function of a complex variable. $\psi(x, y)$ also satisfies Laplace's equation on Ω with the Dirichlet and Neumann boundary conditions interchanged, so $\psi = \psi_{AC}$ and $\psi = \psi_{BD}$ on the lateral sides of the coil. Using conformal mappings [2], the curved domain Ω can be transformed to a rectangular strip, with an expression for resistance in terms of generalized definitions for length and width of the domain in the conformal variables,

$$R = \frac{\phi_{AB} - \phi_{CD}}{\psi_{AD} - \psi_{BC}} = \frac{\text{"Length"}}{\text{"Width"}}. \quad (9)$$

For a rectangular strip aligned with the axes, clearly, length and width can be defined by $L = \Delta x$ and $W = \Delta y$. As described above, by generating an appropriate conformal mapping, the boundaries of Ω are mapped onto level curves of the curvilinear coordinate system given by ϕ and ψ , thus $L = \Delta\phi$ and $W = \Delta\psi$, where ϕ and ψ are locally orthogonal coordinates.

In the following sections we present various solutions to simplified model problems based on several different approaches, including potential theory, geometry and the calculus of variations, multi-scale asymptotics, and finally, computations of a complementary boundary value problem.

3 Direct calculation of the shape optimization problem

One of the most efficient numerical techniques for direct solution of the mixed boundary value problem (1-4) for a given, arbitrarily-shaped simply connected domain Ω is the boundary element method (BEM) [9]. This method follows from the boundary integral representation of the problem,

$$-\phi(\partial\Omega) + \oint_{\partial\Omega} \left(G \frac{\partial\phi}{\partial n} - \phi \frac{\partial G}{\partial n} \right) ds = 0, \quad (10)$$

where the Green's function for Laplace's equation is

$$G(x, y, x', y') = -\frac{1}{2\pi} \ln \sqrt{(x - x')^2 + (y - y')^2}. \quad (11)$$

For a discretization of the solution on the boundary, equation (10) is a system of linear equations for the unknown values of the solution ϕ and its normal derivative $\partial\phi/\partial n$ on the boundary. Using numerical quadrature to evaluate the integrals and linear algebra to solve the matrix system, the solution can be obtained at all points in the domain. Then, the current can be calculated from (5), and the optimal coil shape [8] can be found by repeating this calculation over the set of all feasible domains Ω (see Figure 3).

4 Model solutions

There are very few closed-form exact solutions for the coil resistance problem that can be obtained from potential theory. We considered two models: (i) a coil composed of concentric circular shells and (ii) an exponential spiral coil.

4.1 Concentric circular shells

One geometric simplification that can be made for tightly wound coils is that each turn of the coil is approximately a circular loop. From potential theory, using the function $f(z) = \log z$, the resistance to current flowing in a circular conducting shell with inner radius r^{in} and outer radius r^{out} is

$$R = \frac{2\pi}{\ln(r^{\text{out}}/r^{\text{in}})}. \quad (12)$$

We will assume that the details of the coil structure connecting successive turns do not significantly change the resistance from (12). Given our assumption that the boundaries of the annular domain D are concentric circles, $\Gamma^{\text{out}} : r^{\text{out}} = 1$ and $\Gamma^{\text{in}} : r^{\text{in}} = \bar{r} > 0$ then the individual circular shells are described by

$$r_1^{\text{out}} = 1, \quad r_i^{\text{out}} = r_i^{\text{in}} - d, \quad r_N^{\text{in}} = \bar{r}, \quad i = 1, 2, \dots, N \quad (13)$$

where the turn radii r_i^{in} (decreasing radii with increasing index), for $i = 1, 2, \dots, N$, are unknowns to be determined by minimizing the total resistance

$$R = \sum_{i=1}^N \left[2\pi / \ln(r_i^{\text{out}}/r_i^{\text{in}}) \right]. \quad (14)$$

Carrying out this minimization requires the solution of a system of N nonlinear equations. In general, this process must be carried out numerically, but several insights can be drawn from the calculations:

1. If $\delta = 0$ (or the separation distance is negligibly small compared to the width of the coil turns), then it can be shown that r_i^{in} should be selected to give each turn an equal resistance, $R_i = R/N$. The turn radii are then given by a geometric series, with the total resistance of the coil given by

$$R = \frac{2\pi N^2}{\ln(1/\bar{r})}, \quad r_{i-1}^{\text{out}} = r_i^{\text{in}} = \bar{r}^{i/N}, \quad i = 1, 2, \dots, N \quad (15)$$

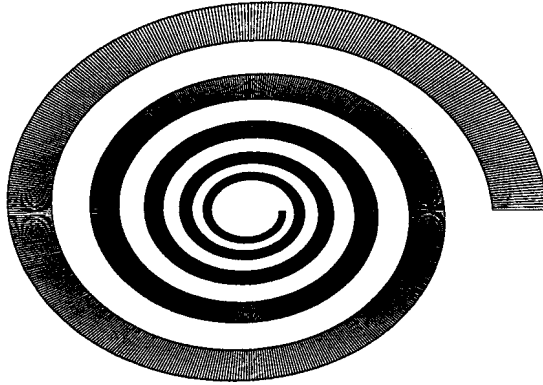


Figure 4: An exponential spiral coil (16) with $N = 5$ turns.

2. More generally, for finite $\delta > 0$, computations show that the coil turns should have unequal resistances, with resistance decreasing as the turn index increases (i.e. the innermost turns have the lowest resistance). Compared to the equal resistance case for $\delta = 0$, the inner turns will have relatively higher resistances while outer turns will have lower resistances and the whole coil will have a higher total resistance. Somewhat counter-intuitively, in the optimum solutions conducting material area is shifted towards the outer turns. This behavior can also be interpreted as shifting area devoted to the lithographic constraint towards the center of the coil.

4.2 Exponential spiral

The geometric model of section (4.1) can be improved by using an exponential spiral for the shape of the coil. The shape of the inner and outer boundaries of the spiral can be derived from the complex function $f(z) = (1 - ib) \log z$,

$$r^{\text{out}}(\theta) = e^{-b\theta}, \quad r^{\text{in}}(\theta) = \bar{r}e^{-b(\theta-2\pi N)}. \quad (16)$$

From potential theory, these equations describe lines of current flow given by a superposition of a vortex and a sink. In general, the separation between successive turns of the spiral will be at least δ if the lithographic constraint is imposed at $\theta = 2\pi N$, $r^{\text{out}}(2\pi N) = r^{\text{in}}(2\pi(N - 1)) - \delta$, or

$$\lambda^{N+1} + \delta\lambda - \bar{r} = 0, \quad \lambda = e^{-2\pi b}. \quad (17)$$

Solving this equation numerically will yield the exact value for the spiral pitch exponent b , which for the limit $\delta \rightarrow 0$ approaches $b \rightarrow \ln(1/\bar{r})/[2\pi(N + 1)]$. The general expression for the resistance of the spiral is then

$$R = \frac{2\pi N^2}{\ln(1/\bar{r}) - 2\pi N b}. \quad (18)$$

For tightly wound spirals with $b \rightarrow 0$, we see that the limit of the set of concentric loops is approached. See Figure 4 for an exponential spiral with $N = 5$ turns.

The above model shows that the current can be viewed as a potential flow of charges in the domain occupied by the coil. In particular, this potential flow and more general coil designs can be generated by distributions of sources, sinks and point vortices, as in the study of problems in fluid dynamics [3].

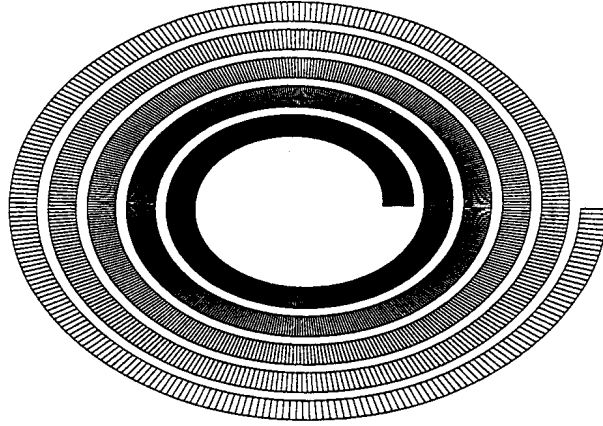


Figure 5: A spiral solution given by equations (23, 24) for a coil with $N = 5$ turns, $r^{\text{in}} = 1$, $r^{\text{out}} = e$, $\sigma = 0.1$, and total resistance $R \approx 5.85$.

5 Geometric optimization

Motivated by the general principle that resistance of a curved domain is given by the ratio of the length to width of the domain (9), we sought spiral domains satisfying this property. Assume that the inner boundary of a very thin, tightly wound spiral coil is given by $r^{\text{in}}(\theta) = g(\theta)$ and the outer boundary is given by $r^{\text{out}}(\theta) = g(\theta - 2\pi) - \delta$, then the resistance of the coil can be taken to be

$$R = \int_0^{2\pi N} \frac{ds}{w} = \int_0^{2\pi N} \frac{\sqrt{g^2 + g'^2} d\theta}{g(\theta + 2\pi) - g(\theta) - \delta}. \quad (19)$$

We can then further approximate this integral by

$$R \sim \frac{1}{2\pi} \int_0^{2\pi N} \frac{g(\theta) d\theta}{g'(\theta) - \sigma}, \quad \sigma = \delta/(2\pi). \quad (20)$$

Using the calculus of variations [11], we derived the Euler-Lagrange differential equation for functions $g(\theta)$ that minimize this integral,

$$g'(\theta)(g'(\theta) - \sigma) - 2g(\theta)g''(\theta) + (g'(\theta) - \sigma)^2 = 0. \quad (21)$$

For $\sigma = 0$, the solutions of this equation are exponential spirals, $g(\theta) = a \exp(b\theta)$. For small σ , we can do a perturbation expansion for $\sigma \rightarrow 0$ to obtain spirals as the expansion

$$g(\theta) \sim e^\theta + \sigma(e^\theta + \theta e^\theta - 3/2) + O(\sigma^2). \quad (22)$$

More generally, we were also able to obtain a parametric solution of (21) in the form

$$g(t) = a\sigma(\cosh t - 1), \quad \theta(t) = a(\cosh t - 1) - a(\sinh t - t) + k, \quad (23)$$

for t in the range $t_0 \leq t \leq t_1$. The four constants, a, k, t_0, t_1 in this solution are determined by the solving a system of four nonlinear equations for the boundary conditions,

$$\theta(t_0) = 0, \quad \theta(t_1) = 2\pi N, \quad g(t_0) = \bar{r}, \quad g(t_1) = 1. \quad (24)$$

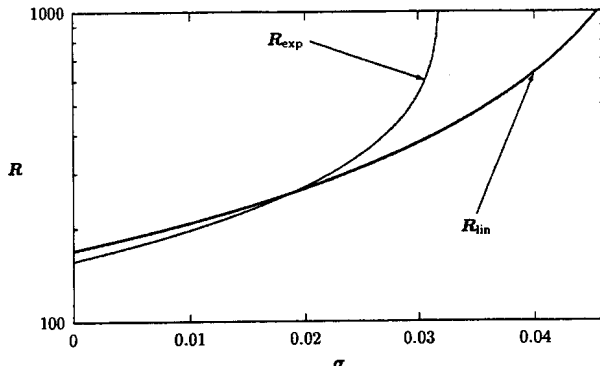


Figure 6: Comparison of the geometric resistances of linear and exponential spirals as a function of the scaled lithographic constraint σ .

5.1 Resistance calculations for elementary spirals

While we have obtained a general solution of equation (21), the parametric representation of the solution (23) and the nonlinear constraints on the constants (24) make insight into the general dependence on design parameters difficult. As an alternative approach, we have also calculated the resistances of simple analytic coil designs, $r = g(\theta)$, from integral (20). These solutions will not globally minimize the resistance integral, but they yield analytic formulas for the resistance that make the dependence on the design parameters (N , the number of turns, and σ , the scaled lithographic constant) clear. We compared two spirals that satisfy the same boundary conditions, $r^{\text{out}} = g(0) = e$ and $r^{\text{in}} = g(2\pi N) = 1$. These two models were the linear and exponential spirals on $0 \leq \theta \leq 2\pi N$,

$$g_{\text{lin}}(\theta) = \frac{e-1}{2\pi N}\theta + 1, \quad g_{\text{exp}}(\theta) = \exp[\theta/(2\pi N)]. \quad (25)$$

Direct substitution into (20) yields

$$R_{\text{lin}} = 2\pi N^2 \ln\left(\frac{e-2\pi N\sigma}{1-2\pi N\sigma}\right), \quad R_{\text{exp}} = 2\pi N^2 \left(\frac{e+1}{2(e-1-2\pi N\sigma)}\right). \quad (26)$$

A plot of these two resistances, for a coil with a fixed number of turns $N = 5$, is shown in Figure 6 as a function of the lithographic constant σ . As can be seen for the graph, for $\sigma \rightarrow 0$, the exponential spiral has the lower resistance, while for larger σ , there is a transition and eventually, the linear spiral has lower resistance for a given, sufficiently large, value of σ .

6 Multi-scale asymptotic solution (Howell)

We now pursue a multi-scale asymptotic [5] solution of the free-boundary problem for Laplace's equation (1–4). This approach formally derives the proper generalization of (9) in the limit of a very slender tightly wound coil.

Consider the limit $N \rightarrow \infty$, with $\delta = O(1/N)$. In this limit, the thickness of the strip tends to zero (like $1/N$) so we can use a “thin layer” approach. Suppose the outer arm of the spiral is given by $r = g(\theta)$ (where $\{r, \theta\}$ are plane polar coordinates). Then to make it match with the given inner and outer boundaries of \mathcal{D} , Γ^{in} and Γ^{out} , we require

$$g(\theta) = r^{\text{in}}(\theta) + O(1/N), \quad \theta \in (0, 2\pi), \quad (27)$$

$$g(\theta) = r^{\text{out}}(\theta) + O(1/N), \quad \theta \in (2(N-1)\pi, 2N\pi), \quad (28)$$

where Γ^{in} and Γ^{out} are given respectively by $r = r^{\text{in}}(\theta)$ and $r = r^{\text{out}}(\theta)$. (For example, we might set $g(\theta) = R_{\text{in}}(\theta) + \delta\theta/(2\pi)$ for $0 < \theta < 2\pi$ and similarly on Γ^{out} .)

At each point of the strip the inner part of the boundary is given by $r = g(\theta)$ and the outer by (say) $r = g(\theta) - \epsilon h(\theta)$ where

$$\epsilon = \frac{1}{N} \ll 1.$$

We can find an expression for $h(\theta)$ as follows. Consider a plane curve given parametrically by $\mathbf{r} = \mathbf{r}_0(s)$. Then the curve lying a distance δ inside is given by $\mathbf{r}_1 = \mathbf{r}_0 - \delta \mathbf{n}$, where \mathbf{n} is the outward-pointing normal to the original curve (in fact the two curves have coincidental normals at corresponding values of s).

For our problem consider the outer boundary of a spiral-shaped strip whose inner boundary is given by $r = g(\theta)$, *i.e.*

$$\mathbf{r} = g(\theta) \begin{pmatrix} \cos \theta \\ \sin \theta \end{pmatrix}.$$

Then the outer boundary is the curve a distance δ inside that given by $r = g(\theta + 2\pi)$. Now, here the unit normal is

$$\mathbf{n} = \frac{1}{\sqrt{g^2 + (g')^2}} \begin{pmatrix} g \cos \theta + g' \sin \theta \\ g \sin \theta - g' \cos \theta \end{pmatrix},$$

so the outer boundary is given parametrically (with parameter $\alpha \approx \theta + 2\pi$) by

$$\mathbf{r} = g(\alpha) \left(1 - \frac{\delta}{\sqrt{g(\alpha)^2 + g'(\alpha)^2}} \right) \begin{pmatrix} \cos \alpha \\ \sin \alpha \end{pmatrix} - \frac{\delta g'(\alpha)}{\sqrt{g(\alpha)^2 + g'(\alpha)^2}} \begin{pmatrix} \sin \alpha \\ -\cos \alpha \end{pmatrix}. \quad (29)$$

This can be written as $\mathbf{r} = (\tilde{g}(\tilde{\theta}) \cos \tilde{\theta}, \tilde{g}(\tilde{\theta}) \sin \tilde{\theta})$, where

$$\tilde{g}^2 = g(\alpha)^2 + \delta^2 - \frac{2\delta g(\alpha)^2}{\sqrt{g(\alpha)^2 + g'(\alpha)^2}}, \quad (30)$$

$$\tan(\tilde{\theta} - \alpha) = \frac{\delta g'(\alpha)}{g(\alpha) [\sqrt{g(\alpha)^2 + g'(\alpha)^2} - \delta]}. \quad (31)$$

Thus we have the following simultaneous equations for $h(\theta)$:

$$g(\theta) + \epsilon h(\theta) = g(\alpha) \sqrt{1 - \frac{2\delta}{\sqrt{g(\alpha)^2 + g'(\alpha)^2}} + \frac{\delta^2}{g(\alpha)^2}}, \quad (32)$$

$$\alpha = \theta + 2\pi - \tan^{-1} \left(\frac{\delta g'(\alpha)}{g(\alpha) [\sqrt{g(\alpha)^2 + g'(\alpha)^2} - \delta]} \right). \quad (33)$$

So setting

$$\delta = \epsilon D, \quad g(\theta + 2\pi) - g(\theta) \equiv \epsilon H(\theta),$$

we obtain the asymptotic form of $h(\theta)$ as $\epsilon \rightarrow 0$:

$$\alpha \sim \theta + 2\pi - \frac{\epsilon D g'(\theta)}{g(\theta) \sqrt{g(\theta)^2 + g'(\theta)^2}} + O(\epsilon^2), \quad (34)$$

$$h(\theta) \sim H(\theta) - \frac{D \sqrt{g(\theta)^2 + g'(\theta)^2}}{g(\theta)} + O(\epsilon). \quad (35)$$

The free-boundary problem for Laplace's equation (1–4) in plane polar coordinates is now given by

$$r^2 \phi_{rr} + r \phi_r + \phi_{\theta\theta} = 0, \quad 0 \leq \theta \leq 2\pi N \quad g(\theta) \leq r \leq g(\theta) + \epsilon h(\theta) \quad (36)$$

subject to the mixed Dirichlet

$$\phi(\theta = 0) = 1, \quad \phi(\theta = 2\pi N) = 0, \quad (37)$$

and Neumann boundary conditions,

$$r^2 \phi_r - r'(\theta) \phi_\theta = 0, \quad 0 < \theta < 2\pi N, \quad \text{on } r = g \text{ and } r = g + \epsilon h. \quad (38)$$

We change variables to $\{\rho, \theta\}$ where

$$r = g(\theta) + \epsilon \rho,$$

and then (36) becomes

$$[(g + \epsilon \rho)^2 + (g')^2] \phi_{\rho\rho} + \epsilon(g + \epsilon \rho) \phi_\rho - \epsilon g'' \phi_\rho - 2\epsilon g' \phi_{\rho\theta} + \epsilon^2 \phi_{\theta\theta} = 0. \quad (39)$$

We have $\partial\phi/\partial n = 0$ on the two edges of the strip and thus

$$g^2 \phi_\rho = g'(\epsilon \phi_\theta - g' \phi_\rho) \quad \text{on } \rho = 0, \quad (40)$$

$$(g + \epsilon h)^2 \phi_\rho = (g' + \epsilon h')(\epsilon \phi_\theta - g' \phi_\rho) \quad \text{on } \rho = h. \quad (41)$$

We pose asymptotic expansions for the dependent variables in powers of ϵ :

$$g \sim g_0 + \epsilon g_1 + \dots, \quad h \sim h_0 + \epsilon h_1 + \dots, \quad \phi \sim \phi_0 + \epsilon \phi_1 + \dots$$

To lowest order, (39–41) simply tell us that ϕ_0 is independent of ρ , *i.e.*

$$\phi_0 = \phi_0(\theta). \quad (42)$$

We must proceed to higher order to find an equation for ϕ_0 . At $O(\epsilon)$ we obtain

$$\phi_1 = A(\theta) + \frac{r g'_0 \phi'_0}{g_0^2 + (g'_0)^2}, \quad (43)$$

where A is as yet arbitrary (again, higher-order terms must be considered to determine A). Finally, the solvability condition of the inhomogeneous Neumann problem for ϕ_2 gives an equation for ϕ_0 , which can be written in the form

$$\frac{d}{d\theta} \left(\frac{g_0 h_0 \phi'_0}{g_0^2 + (g'_0)^2} \right) = 0. \quad (44)$$

We can identify the bracketed term in (44) as the current passing through the strip, and thus to lowest order our optimization problem becomes

$$\min \int_0^{2N\pi} \frac{g_0^2 + (g_0')^2}{g_0 h_0} d\theta, \quad (45)$$

with h_0 given by (35).

Now we pose a multiple-scale ansatz for $g(\theta)$. The motivation for this approach is that successive arms of the spiral are approximately equal, but that their shape must vary slowly between the shape of Γ^{in} and that of Γ^{out} over many periods. Thus we set

$$g(\theta) \equiv G(\theta, \epsilon\theta), \quad (46)$$

where G is periodic with respect to its first argument:

$$G(\theta + 2\pi, \Theta) \equiv G(\theta, \Theta). \quad (47)$$

The boundary conditions (27, 28) for $g(\theta)$ give

$$g_0(\theta) = r^{\text{in}}(\theta), \quad \theta \in (0, 2\pi), \quad (48)$$

$$g_0(\theta) = r^{\text{out}}(\theta), \quad \theta \in (2(N-1)\pi, 2\pi), \quad (49)$$

and thus

$$G_0(\theta, 0) = r^{\text{in}}(\theta), \quad G_0(\theta, 2\pi) = r^{\text{out}}(\theta). \quad (50)$$

Now substituting the ansatz (46) into (35) we find

$$h_0 = 2\pi G_\Theta - \frac{D\sqrt{G^2 + G_\theta^2}}{G}. \quad (51)$$

Note that, for any $f(\theta, \Theta)$ with $f(\theta + 2\pi, \Theta) \equiv f(\theta, \Theta)$,

$$\int_0^{2\pi/\epsilon} f(\theta, \epsilon\theta) d\theta \sim \frac{1}{2\pi\epsilon} \int_0^{2\pi} \int_0^{2\pi} f(\theta, \Theta) d\theta d\Theta.$$

Thus the functional which we must minimize can be written as (now dropping the zero subscript)

$$\min \int_0^{2\pi} \int_0^{2\pi} \frac{(G^2 + G_\theta^2) d\theta d\Theta}{GG_\Theta - \sigma\sqrt{G^2 + G_\theta^2}}, \quad (52)$$

where $\sigma = D/(2\pi)$, subject to the boundary conditions (50) on $\Theta = 0, 2\pi$ and periodicity of G with respect to θ .

This is now a classical minimization problem. Using the calculus of variations, we obtain the Euler-Lagrange equation for the function $G(\theta, \Theta)$ which minimizes (52), although the equation is very complicated in general. However, one can at least verify that it is uniformly elliptic (so long as the spiral thickness h is positive), and thus well-posed as a boundary-value problem. For example in the limit $\sigma \rightarrow 0$ it takes the relatively simple form

$$G_\Theta^2 G_{\theta\theta} - 2G_\theta G_\Theta G_{\theta\Theta} + (G^2 + G_\theta^2) G_{\Theta\Theta} = GG_\Theta^2. \quad (53)$$

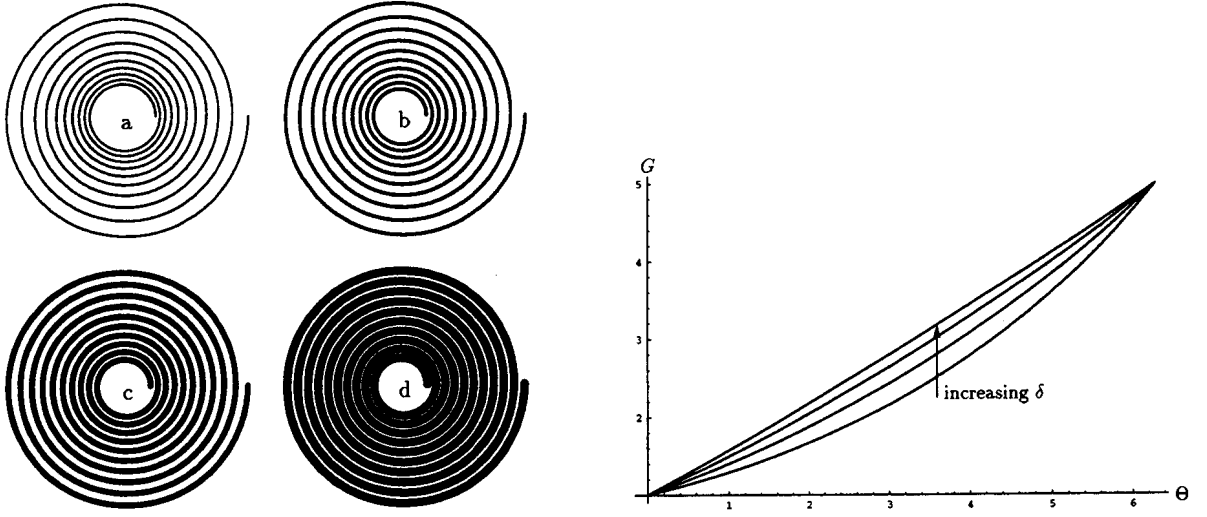


Figure 7: [Left] Optimal circular spiral for number of turns $N = 10$, ratio of radii $\lambda = 5$, scaled gap thickness $\sigma = N\delta/(2\pi) =$ (a)0, (b) $1/(2\pi)$, (c) $1/\pi$, (d) $3/(2\pi)$. White shows the conductor, black the insulator. [Right] Spiral radius G versus scaled angle $\Theta = \theta/N$ for $N = 10$, $\lambda = 5$, $\delta = 0, 1/(2\pi), 1/\pi, 3/(2\pi)$.

Of course, it is alternatively very natural to solve (52) directly using finite elements.

The only hope of analytical progress seems to be when Γ^{in} and Γ^{out} are concentric circles, say

$$R_{\text{in}}(\theta) = 1, \quad R_{\text{out}}(\theta) = \lambda, \quad (54)$$

where $\lambda > 1$ is the ratio of the radii. In this case we can suppose that G is independent of θ and simply minimize

$$\int_0^{2\pi} \frac{G(\Theta) d\Theta}{G'(\Theta) - \sigma}.$$

Since the integrand is autonomous, we can immediately find a first integral of the Euler-Lagrange equation, and thus obtain a first-order ordinary differential equation for $G(\Theta)$:

$$c(G')^2 - 2(G + c\sigma)G' + \sigma(c\sigma + G) = 0, \quad (55)$$

for some constant c . The boundary conditions are

$$G(0) = 1, \quad G(2\pi) = \lambda. \quad (56)$$

Now by setting

$$G = \sigma cf, \quad \Theta = cx,$$

we reduce (55) to a canonical equation for $f(x)$,

$$(f')^2 - 2(f+1)f' + f+1 = 0, \quad (57)$$

whose solution can be written as

$$x = \pm \sinh^{-1}(\sqrt{f}) \mp \sinh^{-1}(\sqrt{a}) + f - a \mp \sqrt{f(1+f)} \pm \sqrt{a(1+a)}. \quad (58)$$

Setting $f(0) = a = 1/(\sigma c)$, the constant a is related to σ and λ by

$$2\pi a \sigma = \pm \sinh^{-1}(\sqrt{\lambda a}) \mp \sinh^{-1}(\sqrt{a}) + (\lambda - 1)a \mp \sqrt{\lambda a(1 + \lambda a)} \pm \sqrt{a(1 + a)}. \quad (59)$$

Now, since $\sigma = N\delta/(2\pi)$, we require $\sigma \leq (\lambda - 1)/(2\pi)$, and this requires us to take the + branch in (58, 59):

$$x = \sinh^{-1}(\sqrt{f}) - \sinh^{-1}(\sqrt{a}) + f - a - \sqrt{f(1+f)} + \sqrt{a(1+a)}, \quad (60)$$

$$2\pi a \sigma = \sinh^{-1}(\sqrt{\lambda a}) - \sinh^{-1}(\sqrt{a}) + (\lambda - 1)a - \sqrt{\lambda a(1 + \lambda a)} + \sqrt{a(1 + a)}. \quad (61)$$

We retrieve $G(\Theta)$ from this using

$$f = aG, \quad x = \sigma a \Theta.$$

When $\sigma = 0$, (60, 61) simply gives an exponential spiral

$$G = \lambda^{\Theta/(2\pi)} \quad \text{when } \sigma = 0, \quad (62)$$

while as σ approaches its maximum value, we obtain a *linear* spiral

$$G = 1 + (\lambda - 1)\Theta/(2\pi) \quad \text{when } \sigma = (\lambda - 1)/(2\pi). \quad (63)$$

These results are consistent with the calculations of the geometric resistance of spirals (20) given in the previous section. We show the variation of $G(\Theta)$ with σ in figure 7. The graphs of G versus Θ are all rather close; this is because $(\lambda - 1)$ is fairly small (the maximum difference between the two extreme spirals is of order $(\lambda - 1)^2/8$). In Figure 7 we show what this optimal spiral looks like when $N = 10$, $\lambda = 5$ and four different values of δ (whose maximum value here is $2/\pi$).

7 Solution of the conjugate boundary value problem (Kunyansky, Peterson, Witelski)

Progress in the shape optimization problem of the minimum resistance coil can be made by considering the boundary value problem for the conjugate field. The solution of problem (1–4) physically represents the electrical potential throughout the coil. The equipotential lines, like those shown in Figure 3, are lines of constant voltage. Current flows along curves that are orthogonal to the equipotentials. The boundary value problem for the streamlines of current flow is

$$\nabla^2 \psi = 0 \quad \text{on } \Omega \quad (64)$$

$$\psi = 0 \quad \text{on } AD \quad (65)$$

$$\psi = 1 \quad \text{on } BC \quad (66)$$

$$\mathbf{n} \cdot \nabla \psi = 0 \quad \text{on } AB \text{ and } CD \quad (67)$$

In this problem, the boundary conditions specify a fixed unit current flow, $I = 1$, and hence the energy integral is proportional to the coil resistance, which we seek to minimize,

$$R = \min_{\Omega} \int \int_{\Omega} |\nabla \psi|^2 dA = \int_{BC} \mathbf{n} \cdot \nabla \psi ds. \quad (68)$$

The minimization is with respect to all possible domains Ω that lie within the annular region \mathcal{D} bounded by Γ^{out} and Γ^{in} , i.e. $\Omega \subset \mathcal{D}$. As described above, resistance will be minimized when the area of Ω is maximized, using all possible area for conducting material. We now formulate a boundary value problem on the annular region \mathcal{D} that produces current streamlines with N turns that naturally conform to the domain and minimize the resistance.

In our approach to the problem we make use of all of the area in the annular domain \mathcal{D} for the turns of the coil Ω , “ $\Omega = \mathcal{D}$ ”, and hence assume that the lithographic constraint is zero, $\delta = 0$. Note that ψ is a C^∞ smooth harmonic function on the simply connected domain Ω . However, within the doubly connected annular domain \mathcal{D} , ψ is **not** continuous – it has jumps of unit magnitude across the boundaries of the coil’s windings. To overcome this difficulty we will re-formulate the problem on \mathcal{D} . First, we connect points B and D by an arbitrary smooth curve S , and divide the doubly connected domain \mathcal{D} into singly connected sub-domains corresponding to the turns of the coil by adding new boundaries $S = S^B = S^E$ as shown in Figure 8a. This divides the coil into N open subdomains

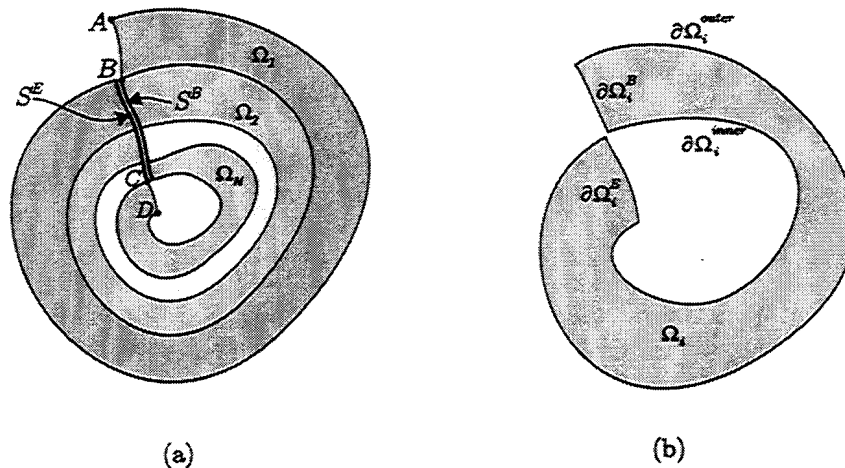


Figure 8: Re-arranging the problem: [Left] (a) splitting the coil [Right] (b) boundaries of a single winding of the coil

$\Omega_1, \Omega_2, \dots, \Omega_N$, where N is the number of windings. Each subdomain Ω_i has a boundary consisting of the four parts $\partial\Omega_i^{\text{beg}}$, $\partial\Omega_i^{\text{end}}$, $\partial\Omega_i^{\text{outer}}$ and $\partial\Omega_i^{\text{inner}}$, defined as shown in Figure ... (b). The solutions $\psi_i(x)$ on each of subdomains Ω_i are harmonic functions satisfying boundary conditions

$$\begin{aligned}\psi_i(x) &= 0, & x \in \partial\Omega_i^{\text{outer}}, \\ \psi_i(x) &= 1, & x \in \partial\Omega_i^{\text{inner}}.\end{aligned}$$

We introduce a function $u(x, y)$ defined by

$$u(x, y) = \psi_i(x, y) + i \quad (69)$$

on each Ω_i . It is easy to see that, unlike $\psi(x)$, function $u(x)$ is continuous across the boundaries of the coil windings. However, now $u(x, y)$ is discontinuous across the ends of each turn, unlike the original streamfunction ψ ; we will introduce jump conditions on u across S . The whole area of the coil may be represented as the domain $\Omega^{\text{comb}} = \bigcup_{i=1}^N \Omega_i$ with the boundary defined by curves $\partial\Omega_1^{\text{outer}}, \partial\Omega_N^{\text{inner}}, S^B, S^E, AB$, and CD . Since $u(x)$ is harmonic in each of the subdomain and continuous by construction, it belongs to the space $H^1(\Omega^{\text{comb}})$. Now the optimization problem may be reformulated in terms of function $u(x)$ and the domain Ω^{comb} as follows: find a subdivision $\Omega_1, \Omega_2, \dots, \Omega_N$

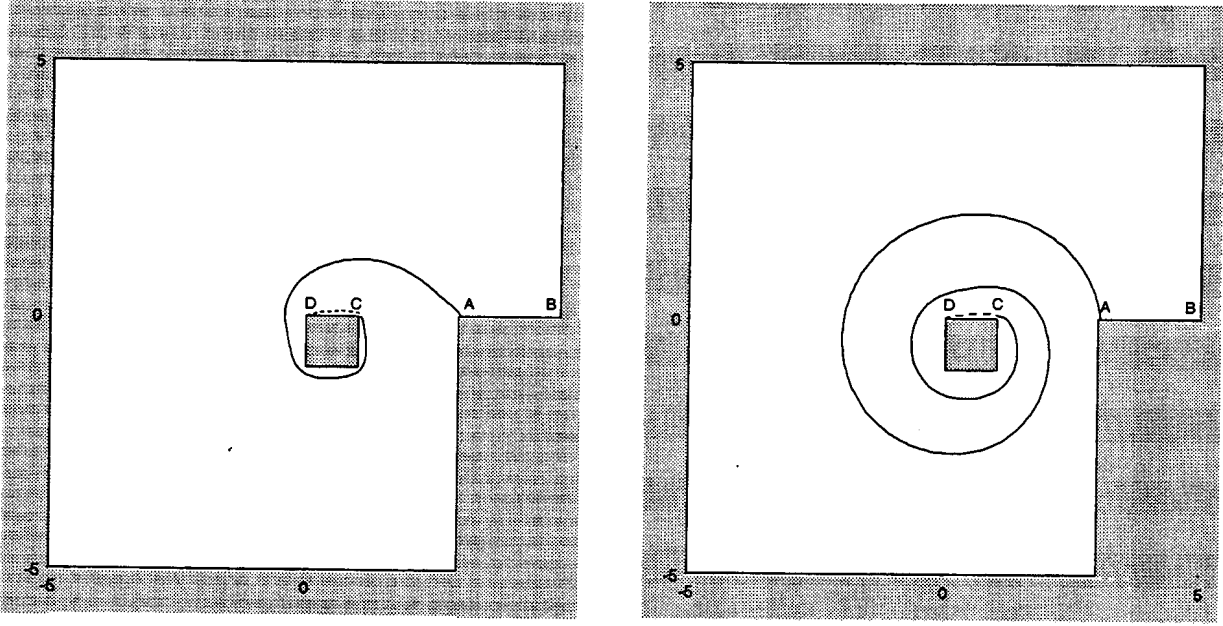


Figure 9: Optimal coil designs for $N = 1$ and $N = 3$ from equations (80–84).

of the Ω^{comb} , such that function $u(x)$ minimizes the Dirichlet functional

$$W_1(\Omega_1, \Omega_2, \dots, \Omega_N) = \iint_{\Omega^{comb}} |\nabla u|^2 d\Omega, \quad (70)$$

where $u(x) \in H^1(\Omega^{comb})$ satisfies the following conditions:

- Harmonic in each subdomain:

$$\nabla^2 u = 0, \quad x \in \Omega_i, \quad i = 1, 2, \dots, N \quad (71)$$

- Dirichlet conditions on the external boundaries:

$$\begin{aligned} u(x) &= 0, & x \in \partial\Omega_1^{outer} \\ u(x) &= N, & x \in \partial\Omega_N^{inner} \end{aligned} \quad (72)$$

- jump conditions on S^E and S^B :

$$u(x)|_{S^B} = 1 + u(x)|_{S^E}, \quad (73)$$

$$\frac{\partial u}{\partial n}|_{S^B} = \frac{\partial u}{\partial n}|_{S^E}, \quad (74)$$

- Neumann conditions in the beginning and the end of the coil:

$$\frac{\partial u}{\partial n} = 0, \quad x \in AB \cup CD, \quad (75)$$

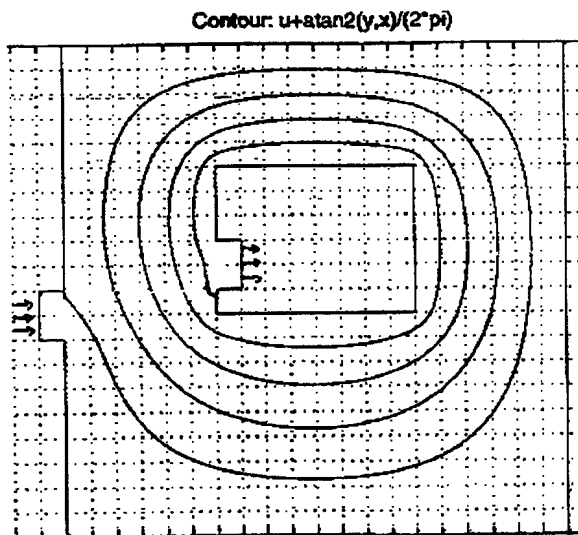


Figure 10: A FEM calculation for an optimal coil with more turns.

- conditions on the winding boundaries:

$$u(x) = i - 1, \quad x \in \partial\Omega_i^{outer}, i = 2, 3, \dots, N. \quad (76)$$

If we can find a subdivision $\Omega_1, \Omega_2, \dots, \Omega_N$ for which function $u(x)$ satisfies conditions (76), this subdivision would be the optimal one. But, such a subdivision is constructed by setting the boundaries $\partial\Omega_i^{outer}$ to be the contour lines $u(x) = i - 1$. Therefore, the (unique) optimal shape of the coil can be found as the set of the constant level curves for the solution $u(x)$ of the Laplace equation with the boundary conditions (72-75).

The above derivation also provides a justification for the equiresistance principle for $\delta = 0$ stated earlier in this Report. Indeed, since the current in the optimal coil is described by a function harmonic in the whole domain, the derivative $\partial\psi/\partial n$ is continuous through the boundaries of the windings. Therefore, the tangential derivative of the potential $\partial\psi/\partial n$ has the same value on the each side of the winding boundary. Integrating along the boundary we see that the difference of the potentials in the beginning and the end of each winding is the same for adjacent windings. This implies that each winding has the same resistance, since the currents through each winding are equal.

We conclude with a simplification of the above procedure that yields our final solution technique. To solve this problem it is necessary to introduce a branch cut, called S above, into the doubly connected domain \mathcal{D} . This can be done in a very standard way through the use of polar coordinates, as in Figure 2b. In polar coordinates, an equivalent definition of $u(x, y)$ in terms of ψ is given by

$$u(x, y) = \psi_i(x, y) + \left[\frac{\theta}{2\pi} \right], \quad (77)$$

where $[x]$ denotes the greatest integer function. As noted above, u must satisfy certain jump conditions across the branch cut S (73, 74). The need for these conditions can be eliminated by introducing the new function

$$v(x, y) = u(x, y) + \{\theta/(2\pi)\} \bmod 1, \quad (78)$$

where $v(x, y)$ is now continuous everywhere inside \mathcal{D} . In fact, $v(x, y)$ is harmonic on \mathcal{D} since it is the sum of two harmonic functions,

$$v(x, y) = \psi(x, y) + \frac{\theta}{2\pi}. \quad (79)$$

Corresponding to problem (64– 67) the boundary value problem for $v(x, y)$ describing an optimal coil with N turns is

$\nabla^2 v = 0$	on \mathcal{D}	(80)
$\frac{\partial v}{\partial n} = \frac{1}{2\pi} \frac{\partial \theta}{\partial n}$	on AB (the current source)	(81)
$\frac{\partial v}{\partial n} = \frac{1}{2\pi} \frac{\partial \theta}{\partial n}$	on CD (the current sink)	(82)
$v(x, y) = \frac{\theta}{2\pi}$	on $\Gamma^{\text{out}} - AB$	(83)
$v(x, y) = \frac{\theta}{2\pi} + N$	on $\Gamma^{\text{in}} - CD$	(84)

where $\theta(x, y) = \tan^{-1}(y/x) \in [0, 2\pi)$. The optimal coil design is then found by using the solution $v(x, y)$ to trace the contour giving the inner boundary of the coil, $\psi = v - \theta/(2\pi) = 1$. Approximate optimal designs calculated with a BEM code, for $N = 1$ and $N = 3$ turns are shown in Figure 9. The same domain \mathcal{D} was used for comparison with Figure 3, the resistance of the design in Fig 9a is **less than half** of the equivalent resistance of the earlier design.

Acknowledgment: We thank M. Williams and I. McFadyen of IBM Storage Systems Division (SSD), San Jose, for suggesting this problem.

References

- [1] Cheng, D. K., Field and wave electromagnetics, 2nd ed, Addison-Wesley, Reading Massachusetts, (1989).
- [2] Churchill, R. V., and Brown, J. W., Complex Variables and applications, 4th ed, McGraw-Hill, New York, (1984).
- [3] Currie, I. G., Fundamental Mechanics of Fluids, McGraw-Hill, New York, (1974).
- [4] Dettman, J. W., Applied complex variables, Dover, New York, (1965).
- [5] Kevorkian, J. and Cole, J. D., Multiple scale and singular perturbation methods, Springer-Verlag, New York, (1996).
- [6] Magid, L. M., Electromagnetic fields, energy, and waves, John Wiley, New York, (1972).
- [7] Mee, C. D., The physics of magnetic recording, North-Holland, New York, (1968).
- [8] Pironneau, O., Optimal shape design for elliptic systems, Springer-Verlag, New York, (1984).
- [9] Ramachandran, P. A., Boundary element methods in transport phenomena, Computational mechanics publications, Elsevier Applied Science, London, (1994).

- [10] Stakgold, I., Green's functions and boundary value problems, Wiley-Interscience, New York, (1979).
- [11] Weinstock, R., Calculus of variations, McGraw-Hill, New York, (1952).